COBEM 2023 27TH INTERNATIONAL CONGRESS OF MECHANICAL ENGENEERING

ABCM Brazilian Society of Mechanical Sciences and Engineering
27th ABCM International Congress of Mechanical Engineering
December 04-08, 2023, Florianópolis-SC, Brazil

COB-2023-0579
NUMERICAL STUDY OF THE SPRAY PATTERN IN HIGH PRESSURE INJECTED ETHANOL

Gustavo Pardini Gouveia Garcia
Guenther Carlos Krieger Filho
Antonio Luiz Pacifico
Polytechnic School of the University of São Paulo, Av. Prof. Mello Moraes, 2231, São Paulo, 05508-030, SP, Brazil.
gustavopgg@usp.br
guenther@usp.br
alpacifi@usp.br

Abstract. *The high pressure direct injection fuel technology has the potential to enhance the control of the combustion process and consequently reduce the consumption of fuel and emissions of pollutants. Such control pass through the atomization process of the fuel spray. Nowadays, the injectors have multi-holes that are capable to inject the fuel in specific regions and directions of the cylinder. The studies in this area count with experimental and the CFD methodology, which have been focused mostly in gasoline and diesel fuels. The Brazilian biofuel, ethanol, has environmental and technical advantages over the gasoline, this motivated this study. The results are validated according to experimental data collected by phase doppler interferometer (PDI) of ethanol spray injected at 100 bar on six hole commercial automotive injector that injects 16.7 miligrams of fuel during 3.5 miliseconds. The characteristics of the spray that are analyzed are the size of the droplets and their velocities. The holes position and directions were obtained from the injector's supplier datasheet. An extensive revision of the literature was made in order to understand and calibrate the models parameters. Simulation results are according to the experimental data, the obtained SMD of the droplets were between 18 μm and 37 μm while the velocities were between 11 m/s and 38 m/s at distances of 50 mm, 65 mm and 80 mm from the injector.*

Keywords: *ethanol spray, phase doppler interferometer, automotive fuel injector*

1. INTRODUCTION

Ethanol is a biofuel that can be produced from sugar-cane, sugar-beet or corn, for example. When these plants are growing, they consume CO_2 from atmosphere so ethanol is almost carbon neutral. It is still produced in small scale compared with the possible demand but the production per area is constantly improving. Furthermore, new production technologies are very promising.

Other positive aspect is that minor changes in the engine need to be done in order to change the project from gasoline to ethanol fuel based. Technically compared to gasoline, the biofuel has advantage characteristics like greater resistance of detonation, greater heat of vaporization and faster laminar flame speed. The first allow engines with higher compression ratio, which leads to greater thermal efficiency, the second can decrease the air/fuel mixture temperature, increasing the volumetric efficiency and reducing knocking and the third allows to delay the ignition, approximating the combustion process to a constant volume process.

The primary atomization is the breakup of the liquid core into ligaments and big droplets. Three mechanisms result in primary atomization: the turbulence of the liquid inside the injector, the cavitation and the aerodynamics forces. Aleiferis et. Al. [1] made an experimental comparison between gasoline and E85 spray formation with some important conclusions that can be extended to pure ethanol. Due to the greater viscosity, for the same flow conditions, ethanol presents lower Reynolds numbers, which means less turbulence. The cavitation is also smaller in ethanol based on smaller vapor pressure and higher surface tension. Finally, the Ohnesorge number used by Reitz and Bracco [2] to classify the primary breakup regimes is smaller for ethanol compared with gasoline and ultimately can lead to different primary breakup regime at lower temperatures. The higher surface tension of ethanol also reduces the gas phase Weber number, which can ultimately lead to different secondary breakup regime.

For the same injection parameters such as nozzle length, diameter, pressure and temperature, ethanol present lower Reynold numbers (ethanol Re=13000 compared to iso-octane Re=25000 at 20ªC), lower liquid Weber numbers (ethanol Wel=36000 compared to iso-octane Wel=41000 at 20 ªC) and these trends continues in higher temperatures. Ethanol also presented lower gas Weber numbers (ethanol Weg=50~75 compared to iso-octane Weg=60~90 at 1 bar atmosphere pressure). For all conditions, ethanol presented larger droplet sizes compared to gasoline, with thinner and more defined spray plumes at lower temperatures.

2. MATERIALS AND METHODS

The methodology applied in this work consists in two steps. First, experimental data was collected by PDI to characterize the spray atomization. Second, the conditions of the experiment were set up in the CONVERGE software and parameters of the CFD simulation models were calibrated in order to achieve similar results based on previous literature.

2.1 Experiment

An automotive commercial fuel injector has been characterized regarding droplet mean diameter, distribution and velocity. The injector has six exit nozzles and hydrated ethanol was injected at 100 bar during 3.5 ms. The next injection occurs after 60 ms, so the frequency of each event is 16.67 Hz. The arrangement of the experiment is shown in the Fig. 1:

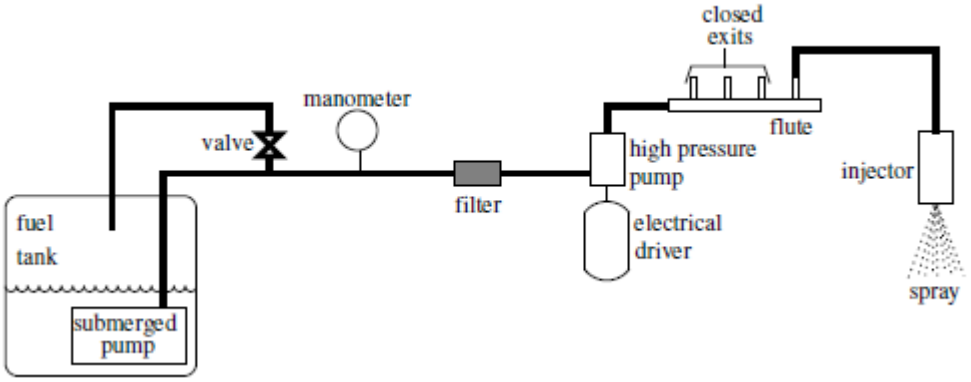

Figure 1. Experimental arrangement for spray control.

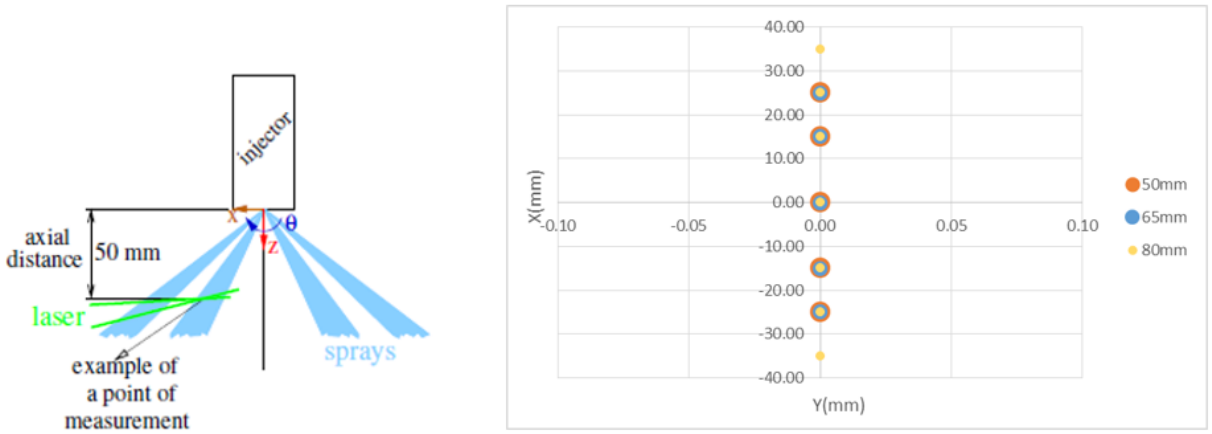

Figure 2. (a) Experimental arrangement for the PDI System measurements. (b) Experimental points of analysis at different distances from injector.

Artium PDI system was used to measure the droplet SMD and its vertical velocity (V_z). The axial distance from the injector was 50 mm as recommended by [3]. The experiment was conducted on open and quiescent atmosphere and the points of measure at 50 mm, 65 mm and 80 mm from injector are illustrated in the Fig. 2(b).

The parameters of the PDI system used were: 500 mm of front focal length, 500 mm of back focal length, slit aperture of 400 µm, collection angle at 38°, beam waist of 312,6 µm and frequency shift of 45 MHz (for Droppler signal sampling).

The acquisition started after 2 ms from the start of the injection and the acquisition time was 3 ms. These times were estimated based on the velocity of the droplets in preliminary tests, so the droplets could reach the measurement point after injection.

The Sauter Mean Diameter (SMD) found were between 23 µm and 28 µm and the velocities in the vertical direction between 14 m/s and 30 m/s.

2.2 CFD Simulation

To understand how fuel properties can affect the atomization phenomenon a CFD simulation using CONVERGE software was done and the results were compared with experimental results from a PDI system.

When the liquid jet encounters the gas phase the atomization process may occur. The simulation used eulerian and lagrangian approaches to simulate the gas and liquid phase respectively.

The next section will briefly explain general models used to the gas and liquid phase. They are called general because their parameters are well defined to match experimental data, so they were applied respecting these relations. Later, the breakup models, which include the observed dimensionless numbers used to classify the atomization regimes, will be detailed and their constants adjusted to according to literature review. Finally, the geometry of the injector and the simulation output configuration will be presented.

2.2.1 General Models

The gas phase is simulated using the eulerean approach because it can be treated as continuous phase and simulate every particle would be very expensive in terms of computational cost. The equations that represents this phase are originated from the principles of the conservation of mass, momentum and energy. These principles generate equations that need to be integrated in space and time, but because of their complexity, they are solved numerically.

In this study, the equations of momentum, species, energy and density are of second order approximation while the turbulence equation is of first order. The PISO method was chose to couple velocity and pressure and the Redlich-Kwong equation of state was used. Turbulence was simulated using the RANS RNG k-ε model. Source terms are included in the equations of the gas phase to represent the interaction with the liquid spray.

The liquid phase can not be treated as continuous but the number of droplets in an automotive spray can make the simulation very computational expensive. To assuage this problem the concept of parcel was adopted. One parcel statistically represents a group of lagrangian droplets that have the same characteristics such as diameter, velocity, temperature and mass.

The equations of this phase comes from the drag phenomenon, the evaporation, the dispersion and finally the atomization.

When the droplet faces the relative velocity of the gas phase, the original spherical shape is deformed until the atomization process happens. This is called the vibrational breakup and the Taylor Analogy Breakup (TAB) model was proposed by O'Rourke e Amsden [4] to simulate it. In this work it is not used as a breakup model but it is used by the dynamic drag coefficient model to account the droplet deformation. The software allows to adjust three constants for dynamic drag coefficient model but this study used the values defined by Lamb [5].

The continuity equation of the gas phase includes a source term to account the addition of mass due to the fuel evaporation process. The evaporation model adopted in this study consider that the droplets are too small that their temperature is uniform and uses the dimensionless Nusselt [6] and Sherwood [7] numbers to represent the heat and mass transfer respectively. The software has defined constants for ethanol and allows the user to change scale factors for heat and mass transfer, but they were used as the default value of one.

The RANS RNG k-Ɛ model includes source terms to account the depletion of turbulent kinetic energy of the gas phase turbulent structures due to the work done to disperse the droplets. In general, the fluctuation velocities in turbulent gas flow leads to quicker and more homogeneous dispersion compared to laminar flow. The change in droplet motion by the interaction with the velocity fluctuation is calculated as a function of total gas velocity (median and fluctuation). Using the O'Rourke turbulent dispersion model, the fluctuation velocities are typically chosen at random value of a Gaussian curve with variance equal to turbulence intensity. The sign of the velocity fluctuation is also chosen by this random value. This process is done for each velocity component at each interaction considering the total velocity of the gas phase at the beginning of the interaction.

Literature review was done for the above models but their constants are defined by experimental data. The last two models used in this study are the Kelvin-Helmholtz and Rayleigh-Taylor breakup models. These two models are the focus of this study and an extensive literature review was done in order to understand and calibrate their constants. The models are presented in the next section.

2.2.2 Kelvin-Helmholtz and Rayleigh-Taylor breakup models

The atomization process in this study considered the Kelvin-Helmholtz and Rayleigh-Taylor break up models applied as secondary breakup once the liquid is injected by blob mode, injecting large droplets with the same radius as the nozzle radius.

The secondary breakup have been classified by the gas Weber number (eq. 6) as in Fig. 3(a). Cited before, the vibrational mode occurs for low Weber numbers and the process divide the droplet in two with the same size. When increasing the relative velocity, the bag mode is reached and two range of sizes is generated, the smaller one from the bag and the bigger one for the rim. If the relative velocity continues to grow, the streamer-shape interior may develop within

the bag, with the resulting droplets with similar size from the rim. Going further, the stripping mode is achieve, resulting in very small droplets that are sheared of the big droplet surface, and then the catastrophic mode is reached for high Weber numbers. It should be noted that more than one mode could be present in engine fuel sprays once the relative velocity varies according to the distance from the nozzle. Also, there are uncertainties about this limits, especially for high Weber numbers.

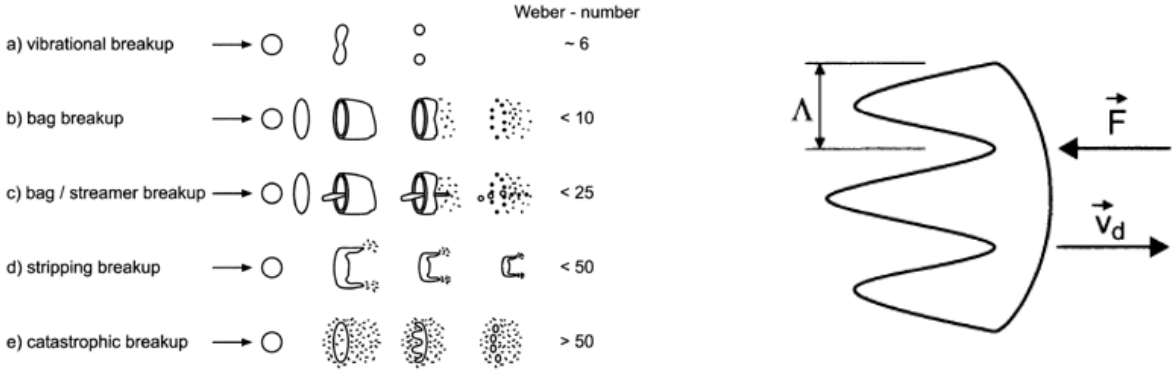

Figure 3. (a) Secondary breakup classification [8]. (b) Rayleigh-Taylor instability scheme.

The Kelvin-Helmholtz also called wave breakup model states that perturbations in the liquid surface due to turbulence or cavitation inside the injector starts to grow when the liquid interacts with the gas phase. Reitz [9] generated numeric solutions to match experimental data and obtained the following expressions for the maximum growth rate Ω and the corresponding wave length Λ:

$$\frac{\Lambda_{KH}}{a} = 9.02\frac{(1+0.45Z^{0.5})(1+0.4T^{0.7})}{(1+0.87We_g{}^{1.67})^{0.6}} \tag{1}$$

$$\Omega_{KH}\left(\frac{\rho_l a^3}{\sigma}\right)^{0.5} = \frac{0.34+0.38We_g{}^{1.5}}{(1+Z)(1+1.4T^{0.6})} \tag{2}$$

In the above equations, a is the nozzle radius, Z is the Onhesorge number, T is the Taylor number and We_g is the Weber number of the gas phase:

$$Z = \frac{We_l{}^{0.5}}{Re_l} \tag{3}$$

$$T = Z\,We_g{}^{0.5} \tag{4}$$

$$We_l = \frac{\rho_l U^2 a}{\sigma} \tag{5}$$

$$We_g = \frac{\rho_g U^2 a}{\sigma} \tag{6}$$

$$Re_l = \frac{Ua}{\nu_l} \tag{7}$$

$$U = u_i + u'_i - v_i \tag{8}$$

In the above equations. u_i is the gas mean velocity, u'_i is the gas fluctuation velocity and v_i is the liquid velocity. If the total relative velocity U increases (We_g increases), the wave length reduces and the growth rate increases. If the liquid viscosity ν_l increases, the growth rate decreases and the wave length increases.

The radius size of the resulting droplet r_c is linearly dependent of the wave length of the fastest growth rate disturbance, with $B_0 = 0.61$ [9]:

$$r_{KH} = B_0\Lambda_{KH} \tag{9}$$

The Kelvin-Helmholtz atomization time is:

$$\tau_{KH} = \frac{3.726 B_1 r_p}{\Lambda_{KH} \Omega_{KH}} \tag{10}$$

For high Weber numbers:

$$\tau_{KH} = B_1 \frac{r_p}{U} \sqrt{\frac{\rho_l}{\rho_g}} \tag{11}$$

In the above equations, B_1 the time constant that can vary from injector to injector. If $B_1 = \sqrt{3}$, the atomization time is equal to TAB model atomization time, but it should be noted that TAB model is applied to vibrational mode while these equations for KH model considers the stripping mode.

The parcel radius r_p is initially equals to nozzle radius. Its variation is described as:

$$\frac{dr_p}{dt} = \frac{(r_p - r_{KH})}{\tau_{KH}} \; for \; r_c \leq r_p \tag{12}$$

In this study, the Kelvin-Helmholtz model allow the creation of new parcels when the initial parcel fragment accumulates after the breakup as following:

$$Ac = \sum_n s N^n \frac{4}{3} \pi \rho_l [(r_p{}^n)^3 - (r_p{}^{n+1})^3] \tag{13}$$

In the above equation, s is a user defined constant between 0% and 100%, that represents the mass fraction contribution of the original parcel to the new parcel and n is the interaction number.

When eq. 13 exceeds the parcel cutoff user defined value (3%~5% of the total injected liquid mass divided by the total number of injected parcels), new parcel of radius r_{KH} is created. The mass conservation is guaranteed by:

$$N^{n+1} (r_p{}^{n+1})^3 = N^n (r_p{}^n)^3 \tag{14}$$

When a new parcel is created, the model add a velocity component normal to the parcel trajectory with $C_n = 0.188$:

$$v_n = C_n \Omega_{KH} \Lambda_{KH} \tag{15}$$

The second model, proposed by Taylor [10], states that when the acceleration and the density gradient has opposite direction, Rayleigh-Taylor instabilities start to grow. For a droplet decelerated by a gas phase, it means that the instabilities will grow in the backside relative to the droplet path, see Fig. 3(b).

The equation that relates the drag force with the droplet deceleration is:

$$\left|F_{drag,i}\right| = m_d |a_i| = m_d \frac{3}{8} C_D \frac{\rho_g |U_i|^2}{\rho_l r_0} \tag{16}$$

Some models neglect the viscosity, but the model presented in CONVERGE considers it once it can have great influence in the atomization process [11]. The growth rate of the greatest instability is given by:

$$\omega_{RT} = -K_{RT}{}^2 \left(\frac{\mu_l + \mu_g}{\rho_l + \rho_g}\right) + \sqrt{K_{RT} \left(\frac{\rho_l - \rho_g}{\rho_l + \rho_g}\right) a_i - \frac{K_{RT}{}^3 \sigma}{\rho_l + \rho_g} + K_{RT}{}^4 \left(\frac{\mu_l + \mu_g}{\rho_l + \rho_g}\right)^2} \tag{17}$$

$$K_{RT} = \frac{2\pi}{\Lambda_{RT}} \tag{18}$$

In the above equations, the frequency of the greatest instability K_{RT} is solved numerically by the bisection method of the eq. 17 and then used to calculate ω_{RT}. The wave length of the wave of the fastest growth rate is given by:

$$\Lambda_{RT} = 2\pi \sqrt{\frac{3\sigma}{|\vec{F}|(\rho_l - \rho_g)}} \tag{19}$$

$$r_{RT} = C_{RT} \Lambda_{RT} \tag{20}$$

$$\tau_{RT} = C_1 / \Omega_{RT} \tag{21}$$

Once again, the breakup size is a linear function of the wave length. If r_{RT} is smaller than droplet diameter, the instability will grow in the drop surface and after the atomization time τ_{RT} the droplet will be atomized by the RT mechanism [12]. C_{RT} and C_1 are user defined constants. The number of new droplets that will be created is defined by the ratio of maximum diameter of the deformed parent droplet to Λ_{RT} and the corresponding diameter of the child droplets is calculates by mass conservation.

To represent the experimental observations and reproduce the intact core of the liquid spray, when using both breakup models together, it is necessary to define a length where only Kelvin-Helmholtz model will atomize the liquid.

$$L_b = C_{bl}\sqrt{\frac{\rho_l}{\rho_g}}d_0 \tag{22}$$

After this length, the KH-RT model will verify if Rayleigh Taylor mechanism can breakup the droplets, if not, the KH model will breakup the droplets again.

For high Weber numbers and $\mu_l = 0$, the KH atomization time is [13]:

$$\tau_{KH} = B_1\frac{r_p}{U}\sqrt{\frac{\rho_l}{\rho_g}} \tag{23}$$

The KH breakup length considering the breakup time of eq. 23 is defined as:

$$L_{KH} = B_1\sqrt{\frac{\rho_l}{\rho_g}}r_0 \tag{24}$$

Comparing eq. 22 and 24, $C_{bl} = 2B_1$. Beale [14] study presented accurate predictions of vaporizing spray penetration when compared to experimental results respecting this relation.

The constants of each equation used in this study are presented in Table 1:

Table 1. Constants of breakup models

Kelvin-Helmholtz Model			
Parameter	Symbol	Equation	Value
Fraction of injected mass/parcel	Ac	13	0.050
Shed mass constant	s	13	1.000
Model size constant	B_0	9	0.610
Model velocity constant	C_n	15	0.188
Model breakup time constant	B_1	11	5.000
Rayleigh-Taylor Model			
Parameter	Symbol	Equation	Value
Model breakup time constant	C_1	21	1.000
Model size constant	C_{RT}	20	0.500
Model breakup lenght constant	C_{bl}	22	10.000

2.2.3 Injector Geometry and position

In order to perform CFD simulation of the spray one has to provide nozzle diameter, Sauter mean diameter of the injection blobs, spray cone angle and position and orientation for each nozzle as shown in Table 2:

Table 2. Nozzle definition parameters

Nozzle	Diameter (m)	SMD (m)	Cone Angle (°)	Position (m)			Orientation (m)		
				x	y	z	x	y	z
1	0.00016	2.9E-05	23	-0.00034000	0.00053899	0.00	-0.00034000	0.00053899	-0.00125071
2	0.00016	2.9E-05	23	0.00034000	0.00053899	0.00	0.00034000	0.00053899	-0.00125071
3	0.00016	2.9E-05	23	-0.00059377	0.00004575	0.00	-0.00059377	0.00004575	-0.00085050
4	0.00016	2.9E-05	23	0.00059000	0.00004562	0.00	0.00059000	0.00004562	-0.00084512
5	0.00016	2.9E-05	23	-0.00033035	-0.00034423	0.00	-0.00033035	-0.00034423	-0.00178057
6	0.00016	2.9E-05	23	0.00033035	-0.00034413	0.00	0.00033035	-0.00034413	-0.00178030

SMD value is the average experimental SMD measured by PDI. The diameter, position and orientation was obtained in the injector datasheet. A free CAD software was used to define nozzle position and orientation according to datasheet instructions. The spray cone angle was adjust based on simulations results, with a bigger spray angle resulting in a lower vertical velocity and smaller SMD.

2.2.4 Phase Doppler Particle Analyzer (PDPA) settings

In CONVERGE, the PDPA is an output tool that can be activated to return parcels velocity and size like the experimental PDI. The user have to define the normal of the plane used for the analysis, the radius around point (volume of analysis), the start time for analysis, the period time to write the output and the location points of the analysis. The location of the points of analysis are indicated in Fig. 2(b) and the other parameters summarized in the Table 3:

Table 3. PDPA parameters

Normal of the plane of analysis	(x=0, y=0, z=1)
Radius of analysis	0.002 m
Start time for analysis	0.065 s
Time interval for output	0.06 s

3. RESULTS AND DISCUSSION

Eleven cycles were simulated with domain size of 0,3m x 0,3m x 0,3m to guarantee that recirculation of the spray were considered during the simulation. The base grid of 3mm was used and grid refinement to verify grid convergence was only made in the spray region to save computational cost using the fixed embedding tool of CONVERGE. Scale parameter equals 1 means that each side of the cell will be divided by 2, cell volume will be divided by 8 in embedding cells, radius 1 is larger than nozzle diameter and the embedding length is almost half of domain and 50% bigger than furthermost PDI measurement point.

Table 4. Fixed embedding parameters

Parameter	Value
Entity type	Injector
Mode	Cyclic
Period	0.06 s
Scale	1
Start time	0.000
End time	0.015
Radius 1	0.0002
Radius 2	0.04
Length	0.12

As pointed out in many studies, when using eularian-lagrangian approach it is not possible to achieve mesh independence. When using eularian approach, grid refinement enhance the discretization, approximating the problem to the real continuous phase, but when the lagrangian approach is used together, points of mass (or any other property) will appear in the middle of the cells and this does not represent continuity. Senecal Et. Al [15] concluded that grid convergence should be the goal of spray studies using this approach. Thus, in order to verify the robustness of the simulation, integral properties of the phenomenon should be used, in the case of liquid sprays, this may be spray penetration. In complement, as any other CFD simulation, it is important to analyze the convergence between cycles to achieve steady state and check if the gas phase properties are in agreement with liquid phase properties.

To test this convergence, some parameters like number injected drops, mass injected and spray penetration were analyzed and presented in Fig. 4 and Fig. 5.

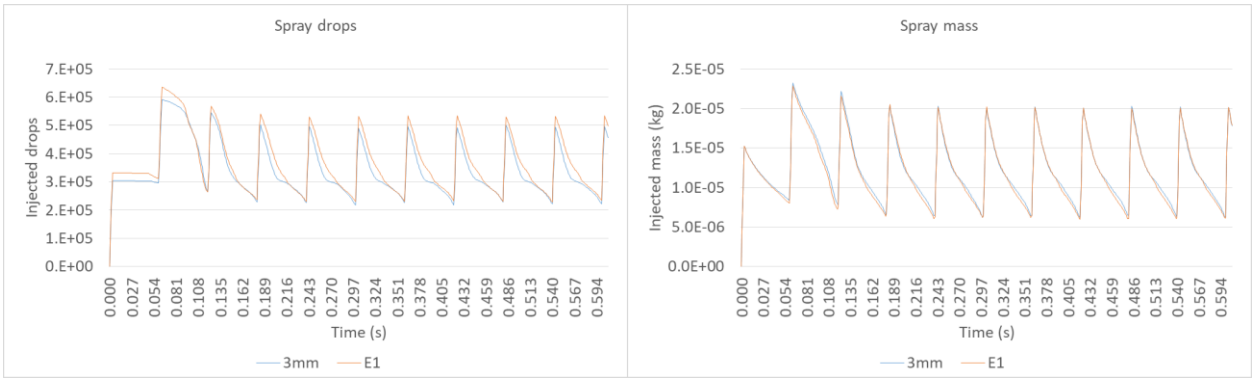

Figure 4. (a) Injected drops in domain. (b) Injected mass in domain.

Figure 5. (a) Spray penetration 95% of liquid mass. (b) Spray penetration 90% of liquid mass.

Fig. 4 shows that simulation achieved steady state between spray cycles and good convergence between the two mashes. Because of the big domain and as the spray velocity reduces with time, the liquid mass stays above zero once before all the liquid leaves the domain the next spray event occurs. Figure 5 shows the spray penetration considering 90% and 95% of total injected liquid mass with good agreement between the two mashes.

The comparison between PDPA simulation results and PDI experiment are present in Fig. 6, Fig. 7 and Fig. 8.

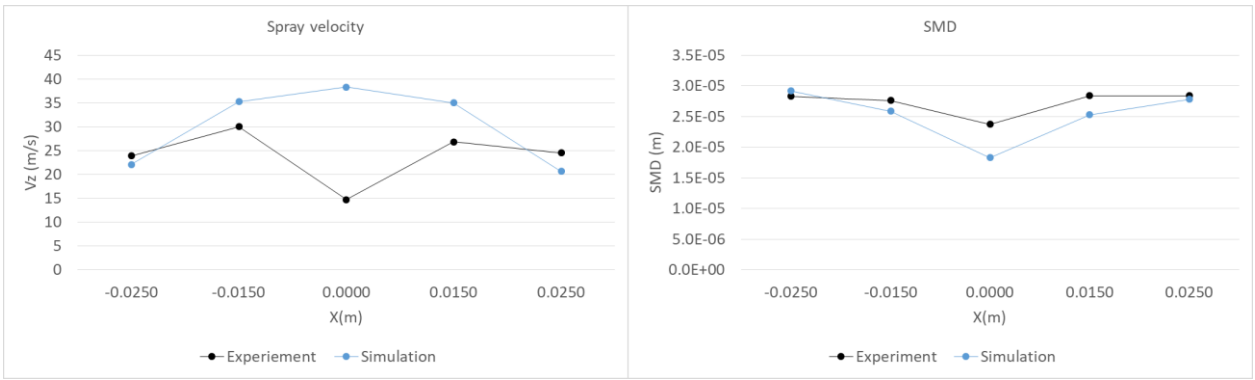

Figure 6. (a) Velocity results at 50mm. (b) SMD results at 50 mm.

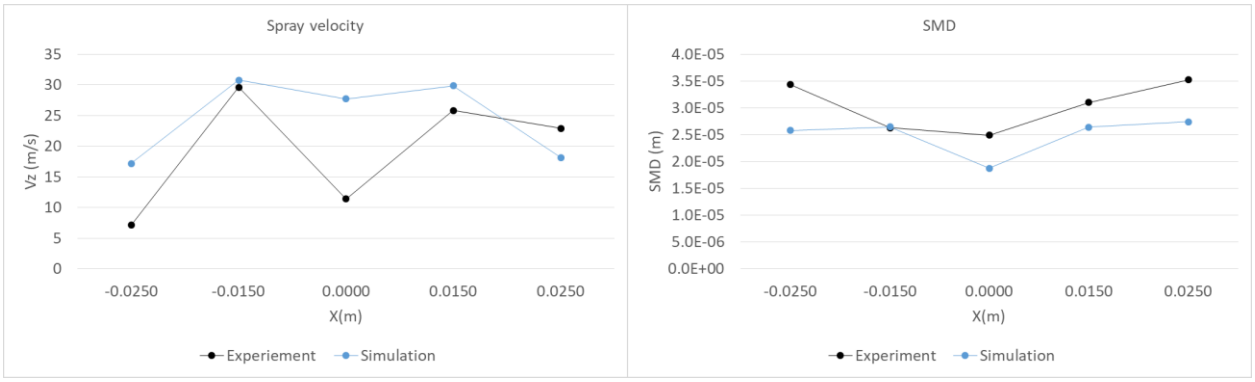

Figure 7. (a) Velocity results at 65mm. (b) SMD results at 65 mm.

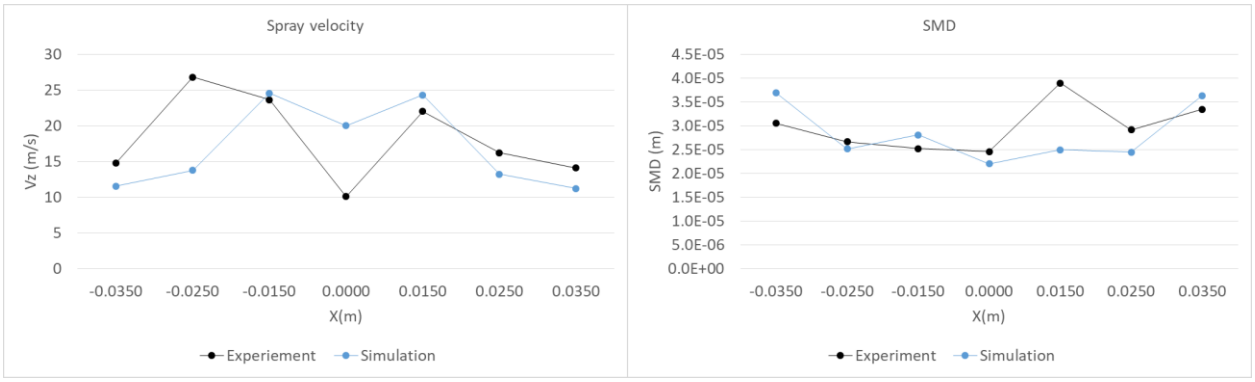

Figure 8. (a) Velocity results at 80mm. (b) SMD results at 80 mm.

Although the simulation results present considerable differences when compared with the experiment, it is important to note that experiment results also have their own errors, which were not analyzed in this study.

4. CONCLUSION

The experiment using PDI measured the spray velocity and droplets SMD in three different planes from the nozzle at various points. The CFD simulation used the eularian approach to simulate the gas phase and the lagrangian approach to simulate the liquid spray. Models used in the simulation considered the drag phenomenon, evaporation, turbulence, dispersion and finally the spray break up models, which literature was analyzed in detail in order to understand and calibrate the parameters.

As grid independence can not be achieved when using eularian-lagrangian approach, the grid convergence was proved using the liquid spray penetration with good agreement between meshes sizes.

The simulation droplets SMD results were close to experiment results for most of the points in the three planes analyzed. The simulation velocities results have some considerable differences when compared to experiment results, mostly in the central region of the spray and more noticed in the planes closer to the injector.

The spray simulation study proved to be robust and the models used in this study can be applied as an initial step to calibrate combustion modelling of further engine simulation.

5. REFERENCES

[1] P.G. Aleiferis a,*, J. Serras-Pereira a, Z. van Romunde a, J. Caine b, M. Wirth c, Mechanisms of spray formation and combustion from a multi-hole injector with E85 and gasoline, 2009.

[2] R.D. Reitz, F.V. Bracco, Mechanisms of atomization of a liquid jet, Physics of Fluids 25 (1982) 1730–1742.

[3] Hung, D.L.S., Harrington, D.L., Gandhi, A.H., Markle, L.E., Parrish, S.E., Shakal, J.S., Sayar, H., Cummings, S.D., Kramer, J.L., " Gasoline fuel injector spray measurement and characterization - A new SAE J2715 recommended practice", SAE Technical Paper Series 2008-01-1068, 2008.

[4] O'Rourke, P.J. and Amsden, A.A., "The TAB Method for Numerical Calculation of Spray Droplet Breakup," SAE Paper 872089, 1987.

[5] Lamb, H., Hydrodynamics, Sixth Edition, Dover Publications, New York, 1945.

[6] Faeth, G.M., "Current Status of Droplet and Liquid Combustion," Progress in Energy and Combustion Science, 3(4), 191-224, 1977. DOI: 10.1016/0360-1285(77)90012-0.

[7] Amsden, A.A., O'Rourke, P.J., and Butler, T.D., "KIVA-II: A Computer Program for Chemically Reactive Flows with Sprays," Los Alamos National Laboratory Technical Report LA-11560-MS, 1989.

[8]Wierzba A (1993) Deformation and Breakup of Liquid Drops in a Gas Stream at Nearly Critical Weber Numbers. Experiments in Fluids, vol 9, pp 59-64

[9] Reitz, R.D., "Modeling Atomization Processes in High-Pressure Vaporizing Sprays,"Atomisation and Spray Technology, 3(4), 309-337, 1987.

[10] Taylor GI (1963) The Shape and Acceleration of a Drop in a High Speed Air Stream. in: Batchelor GK, The Scientific Papers of GI Taylor, vol 3, pp 457--464, University Press, Cambridge.

[11] Senecal, P.K., Richards, K.J., Pomraning, E., Yang, T., Dai, M.Z., McDavid, R.M., Patterson, M.A., Hou, S., and Shethaji, T., "A New Parallel Cut-Cell Cartesian CFD Code for Rapid Grid Generation Applied to In-Cylinder Diesel Engine Simulations," SAE Paper 2007-01-0159, 2007. DOI: 10.4271/2007-01-0159

[12] Xin, J., Ricart, L., and Reitz, R.D., "Computer Modeling of Diesel Spray Atomization and Combustion," Combustion Science and Technology, 137(1-6), 171-194, 1998. DOI: 10.1080/00102209808952050

[13] Senecal, P.K., "Development of a Methodology for Internal Combustion Engine Design Using Multi-Dimensional Modeling with Validation Through Experiments," Ph.D. Thesis, University of Wisconsin-Madison, Madison, WI, 2000.

[14] Beale, J.C., "Modeling Fuel Injection using the Kelvin-Helmholtz/Rayleigh-Taylor Hybrid Atomization Model in KIVA-3V," M.S. Thesis, University of Wisconsin-Madison, Madison, WI, United States, 1999.

[15] Senecal, P.K, "Grid-Convergent Spray Models for Internal Combustion Engine Computational Fluid Dynamics Simulations", Journal of Energy Resources Technology, 2014, DOI: 10.1115/1.4024861

6. RESPONSIBILITY NOTICE

The author are the only responsible for the printed material included in this paper.